


Article

# Structural Origin of Anisotropic Thermal Expansion of Molecular Crystals and Implication for the Density Rule Probed with Four ROY Polymorphs

Sayantan Chattoraj<sup>1,2</sup> and Changquan Calvin Sun<sup>1,\*</sup> 

<sup>1</sup> Pharmaceutical Materials Science and Engineering Laboratory, Department of Pharmaceutics, University of Minnesota, Minneapolis, MN 55455, USA

<sup>2</sup> Process Engineering and Analytics, Drug Product Development, GSK, Collegeville, PA 19426, USA

\* Correspondence: sunx0053@umn.edu; Tel.: +1-612-624-3722

**Abstract:** The objective of this work was to investigate the molecular origin of the differences in the thermal expansivity of four ROY polymorphs (Y, R, OP, and ON) using variable temperature single crystal X-ray diffractometry (VT-SCXRD). Thermal expansivity was found to be directly influenced by the crystal packing and the number and type of directional interactions, such as hydrogen bonds, involved in packing. Polymorphs with layered molecular packing, i.e., ON, OP, and R, show higher volume expansivity, where the axial component of the expansion is the largest in the directions perpendicular to the hydrogen-bonded layers and the smallest along the layers. Polymorph Y shows the least volume expansivity, which corresponds to the presence of a denser hydrogen-bonded network structure in the crystal, and absence of apparent molecular layers. The largest overall expansivity is observed for polymorph ON that lacks intermolecular hydrogen bonds and exhibits a layered packing pattern along two axes. The differences in the thermal expansivity of the ROY polymorphs lead to violations of the density rule in polymorph stability prediction due to crossover in crystal density with change in temperature, which means the rank order of crystal density of polymorphs is temperature-dependent. Thus, at absolute zero, the most thermodynamically stable polymorph Y is predicted to not have the highest density, which violates the density rule. Likewise, for all enantiotropic polymorphs undergoing the density crossover phenomenon, the density rule is valid only within the temperature range bracketed by the temperatures of density crossover ( $T_d$ ) and thermodynamic transition ( $T_t$ ). For all monotropic polymorphs, the density rule is valid only above  $T_d$ .

**Keywords:** thermal expansion; polymorphs; density; thermodynamic stability; crystal packing; solid-state chemistry; thermally induced lattice changes



**Citation:** Chattoraj, S.; Sun, C.C. Structural Origin of Anisotropic Thermal Expansion of Molecular Crystals and Implication for the Density Rule Probed with Four ROY Polymorphs. *Crystals* **2023**, *13*, 270. <https://doi.org/10.3390/cryst13020270>

Academic Editors: Duane Choquesillo-Lazarte and Alicia Dominguez-Martin

Received: 9 January 2023

Revised: 29 January 2023

Accepted: 30 January 2023

Published: 4 February 2023



**Copyright:** © 2023 by the authors. Licensee MDPI, Basel, Switzerland. This article is an open access article distributed under the terms and conditions of the Creative Commons Attribution (CC BY) license (<https://creativecommons.org/licenses/by/4.0/>).

## 1. Introduction

Polymorphism, a phenomenon where the same molecule(s) crystallize in more than one solid phase, is a well-studied phenomenon in solid-state chemistry [1–3]. Polymorphism in pharmaceutical molecules has been extensively investigated because of its relevance to solid form selection for the development of robust drug products [2,4]. Different polymorphs may exhibit differences in thermodynamic, crystallographic, spectroscopic, kinetic, thermal, surface, and mechanical properties [4–8]. While many physical properties of polymorphs have been extensively studied, the thermal expansivity of molecular crystals has received relatively less attention. Thermally induced volume expansion of crystal is a consequence of faster thermal vibrations of molecules with increasing temperature [9], resulting in atoms populating the asymmetric portions of the potential energy-well, which causes changes in bond lengths [10]. Bond angles in a molecule may also vary with temperature [11] to accord with the new force equilibrium among atoms. Negative thermal expansivity (NTE) of molecular crystals can occur, but to a lesser extent than positive

thermal expansivity (PTE) [12,13]. In addition, there have been reports of zero thermal expansivity (ZTE) in some crystals attributed either to isotropic bonding strength in the lattice or the mutual cancellation of positive and negative expansivities in a crystal [14,15]. The packing of molecules in organic crystals is typically anisotropic. Therefore, the thermal expansion behavior in molecular crystals is also expected to be anisotropic, i.e., unit cell dimensions do not all change proportionately with temperature. Studies correlating crystal packing with thermal expansion in molecular crystals are relatively few [16] compared to other classes of crystals, such as metallic and inorganic systems [9]. In addition to pharmaceuticals, thermal expansion of molecular crystals is of interest in the fields of geology, cosmochemistry [17,18], and polymer sciences [19].

The stability relationship among polymorphs may be predicted from their densities, where a polymorph with a lower density is thought to be less stable at absolute zero (the density rule) [20,21]. The most reliable understanding of relative stability relationships among polymorphs is obtained from the free energy–temperature ( $G$ - $T$ ) phase diagram, which may be mapped using heat capacity [22], solubility or dissolution [23,24], heat of solution/transition [20,21], melting [20,21,25], and eutectic melting data [26,27]. The density rule has the advantage of easy data collection, e.g., by calculation from single crystal structure and/or helium pycnometry measurement, but does not always lead to accurate predictions of stability relationship at room temperature. If the relative rank order of the polymorph densities changes with temperature, an application of the density rule at different temperatures of interest would necessarily risk erroneous stability predictions.

The objectives of the present study are twofold: (a) to investigate the molecular origin of the observed differences in thermal expansivity of polymorphic molecular crystals through a careful evaluation of their molecular packing as a function of temperature; and (b) to critically examine the impact of thermal expansivity of polymorphs on the validity of the density rule.

## 2. Materials and Methods

### 2.1. Materials

Four polymorphs of 5-Methyl-2-[(2-nitrophenyl)amino]-3-thiophenecarbonitrile (Figure 1, commonly known as ROY for the red, orange, and yellow colors of polymorphs), yellow prisms (Y,  $T_m$ ~383 K), red prisms (R,  $T_m$ ~378 K), orange prisms (OP,  $T_m$ ~386 K), and orange needles (ON,  $T_m$ ~389 K) were used in this study because of their known thermodynamic stability relationships. Among the six possible pairs of these four ROY polymorphs, Y–R is a monotropic pair, while the other five pairs are enantiotropic with phase transition temperatures ( $T_t$ ) of ~341 K, ~346 K, ~332 K for Y–ON, Y–OP, ON–OP pairs, respectively [26,28]. The  $T_t$  values for the remaining two polymorph pairs, R–OP and R–ON, have not been definitively established, but are predicted to be below room temperature.

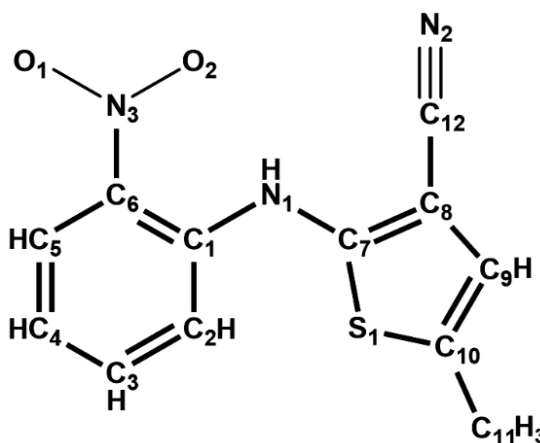


Figure 1. Molecular structure of ROY.

OP crystal seeds were first obtained by evaporating an acetone solution of ROY in an aluminum pan at room temperature. An ethanolic solution of ROY was prepared by dissolving 68 mg ROY in 5 mL ethanol at 60 °C under controlled stirring and the solution was cooled to room temperature. To a portion of this supersaturated solution, the OP seed crystals were added, and the tightly closed vial was left on a bench undisturbed. Large OP single crystals formed after overnight storage were harvested. For the preparation of the other polymorphs, the remaining portion of the ethanolic ROY solution was stored in a tightly closed vial at room temperature. A mixture of polymorphs Y, R, and ON crystals were formed after 19 h, which were manually separated based on crystal color and morphology.

## 2.2. Methods

### Thermal Expansivity Measurements

Thermal expansion of the polymorphs was measured using variable temperature–single crystal X-ray diffraction (VT-SCXRD). VT-SCXRD is advantageous over other approaches, such as interferometry, capacitance dilatometry, and low temperature dilatometry, because VT-SCXRD yields structural information critical for understanding the observed expansion of the crystals. VT-SCXRD data on the polymorphs were collected at four temperatures over 123–273 K temperature range using a Bruker SMART diffractometer (Bruker AXS, operated at 40 kV and 50 mA) equipped with an APEX II CCD detector and using Mo- $K_{\alpha}$  radiation (0.71073 Å) filtered with a graphite monochromator. Single crystals were glued to goniometer glass fiber tips with epoxy adhesive. Data were collected between 5° and 75°  $\theta$  using  $\omega$  and  $\phi$  scans with 0.5° scan width. Beam exposure times varied between 5 and 30 s, depending on the nature and quality of crystals. Diffraction data were integrated to the same resolution (0.77 Å) for all crystals. To eliminate variations in diffraction data due to different crystal quality, the same crystal was used for each polymorph at all temperatures. Temperature was controlled with a temperature controller (Cryostream Controller 600, Oxford, UK) fitted with a CFT-25 refrigerated recirculator (set at 9 psig) to deliver liquid nitrogen. After the data collection at a temperature was completed, the temperature was increased at a ramp rate of 6 K/min to the next highest target temperature and held for 15 min before data acquisition. Full structures of the polymorphs were obtained at multiple temperatures (Tables S1–S13). Polymorph ON yielded very thin needles (<0.4 mm width), so full structure was only solved at 123 K in this study, as satisfactory structure solutions at higher temperatures could not be obtained. Hence, the structure of ON at room temperature (QAXMEH) was obtained from CCDC. Only unit cell parameters were determined at other temperatures for polymorph ON.

## 3. Results

### 3.1. Thermal Expansivity of ROY Polymorphs

For all four polymorphs, the crystal unit cell volumes increase linearly with increasing temperatures. The isobaric volumetric thermal expansion coefficient or expansivity ( $\alpha_v$ ) is the temperature derivative of volume dilation at constant pressure (Equation (1)) [9].

$$\alpha_v = \frac{(\delta V / \delta T)_p}{V} \quad (1)$$

The  $\alpha_v$  value was calculated at a given temperature using the crystal unit cell volume ( $V$ ) at that temperature and the slope of the volume–temperature plot ( $\delta V / \delta T$ ). Thermal expansivity normalizes the effect of the cell volumes on the extent of volume expansion with temperature. Thus,  $\alpha_v$  is a more appropriate parameter for comparing thermal expansion among different crystals instead of the rate of change in volume with temperature,  $\delta V / \delta T$ . The  $\alpha_v$  values for all four ROY polymorphs decrease linearly with increasing temperature within the temperature range probed (Figure 2). The  $\alpha_v$  of polymorph Y at all temperatures is consistently smaller than the other three polymorphs, while polymorph ON consistently shows the largest  $\alpha_v$ .

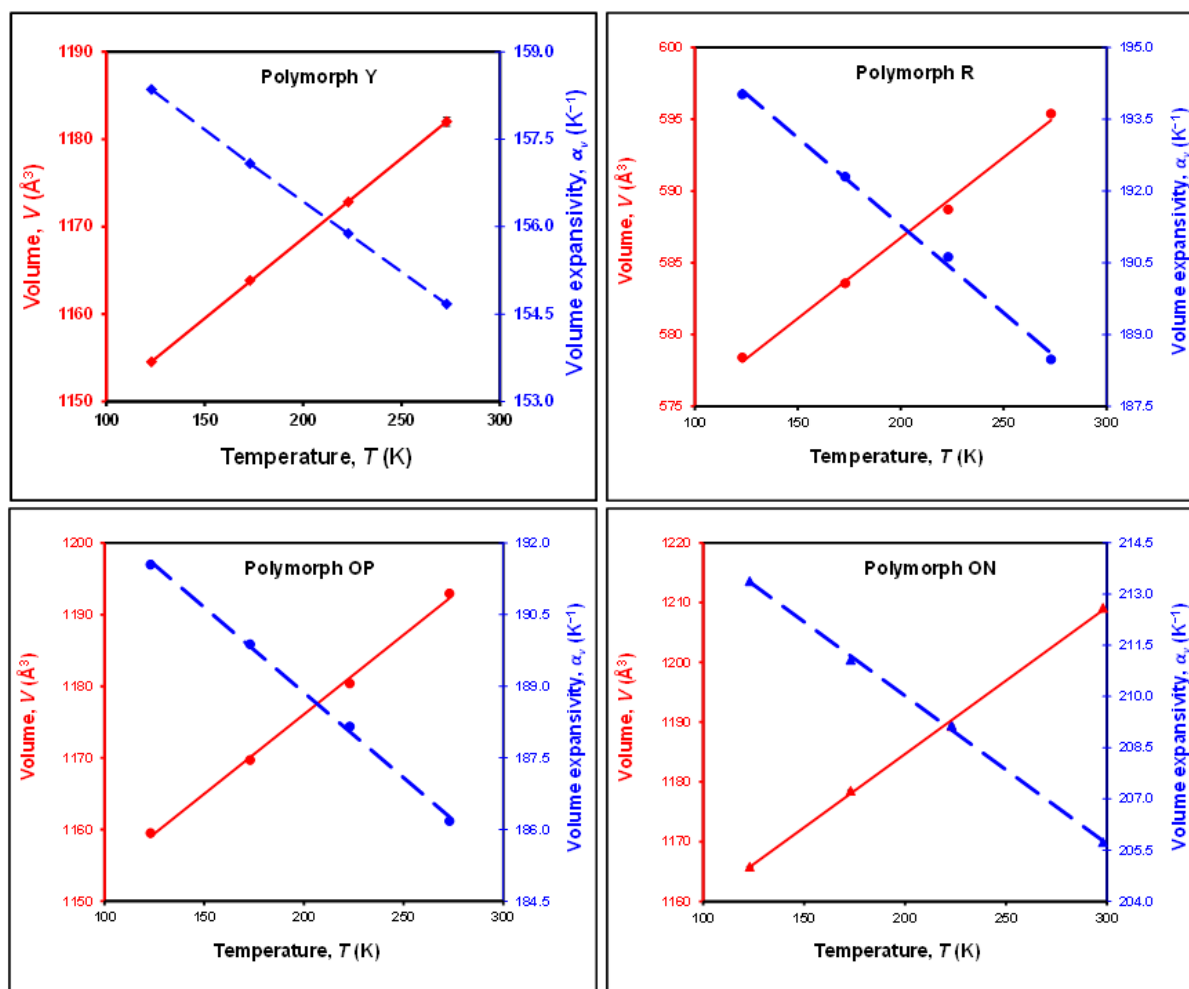


**Figure 2.** Variations of unit cell volume ( $V$ ; solid line) and volume expansivity ( $\alpha_v$ ; dotted line) with temperature for Y, R, OP, and ON polymorphs. At all temperatures,  $\alpha_v$  is the smallest for polymorph Y, and the largest for polymorph ON.

The expansivities along different crystallographic axes and angles are summarized in Table 1. An analysis of axial and angular expansivity provides information for identifying the lattice component of a crystal structure making the greatest contribution to the overall volume expansivity of a crystal. For all four polymorphs, the three axes,  $a$ ,  $b$ , and  $c$ , undergo linear expansion with increase in temperature. However, expansion along different cell axes in each polymorph is highly anisotropic. Anisotropy in thermal expansivity is common in molecular crystals, including polymorphs [29–32]. For polymorph Y, the maximum axial expansivity occurs in the direction of the  $b$  axis, while the maximum expansivities of polymorphs R, OP, and ON all occur along the  $a$  axis.

Angular expansivity for monoclinic polymorphs Y, OP, and ON is restricted to 1 unit cell angle,  $\beta$ , while the other two angles remain invariant ( $90^\circ$ ) with changing temperature. The angle  $\beta$  for all three polymorphs undergo positive thermal expansion with increasing temperature. Expansivity for angle  $\beta$  is the smallest for polymorph Y, and the largest for polymorph ON. For triclinic polymorph R, all three unit cell angles varied with temperature, where angle  $\beta$  expansion is accompanied by contraction in angles  $\alpha$  and  $\gamma$  (NTE). Unit cell angle  $\gamma$  shows the largest absolute expansivity among the three angles in polymorph R.

**Table 1.** Axial and angular expansivities of different ROY polymorphs. The direction of maximum expansivity is highlighted in bold for each polymorph.

Polymorph	Temperature (K)	Crystal System	Axial Expansivity <sup>a</sup> × 10 <sup>−6</sup> (K <sup>−1</sup> )			Angular Expansivity <sup>b</sup> × 10 <sup>−6</sup> (K <sup>−1</sup> )		
			<i>a</i>	<i>b</i>	<i>c</i>	$\alpha$	$\beta$	$\gamma$
Y	123	Monoclinic	13.80	<b>133.72</b>	34.41	Invariant	22.78	Invariant
	173		13.79	<b>132.98</b>	34.34		22.74	
	223		13.79	<b>132.19</b>	34.29		22.71	
	298		13.76	<b>130.75</b>	34.20		22.69	
R	123	Triclinic	<b>135.44</b>	78.90	14.32	−8.306	25.20	−73.37
	173		<b>134.64</b>	78.62	14.31	−8.308	25.17	−73.59
	223		<b>133.79</b>	78.33	14.30	−8.311	25.14	−73.86
	273		<b>132.73</b>	77.97	14.29	−8.316	25.10	−74.18
OP	123	Monoclinic	<b>174.66</b>	13.023	18.14	Invariant	30.95	Invariant
	173		<b>173.31</b>	13.010	18.13		30.92	
	223		<b>171.85</b>	13.003	18.11		30.87	
	273		<b>170.19</b>	12.997	18.09		30.81	
ON	123	Monoclinic	<b>131.73</b>	51.67	20.13	Invariant	72.80	Invariant
	173		<b>130.94</b>	51.49	20.10		72.53	
	223		<b>130.19</b>	51.34	20.09		72.25	
	298		<b>128.76</b>	51.22	20.07		71.89	

<sup>a</sup> Axial expansivity =  $\frac{(\delta l/\delta T)_P}{l}$  where *l* = length of cell axis; <sup>b</sup> Angular expansivity =  $\frac{(\delta \theta/\delta T)_P}{\theta}$  where  $\theta$  = cell angle.

### 3.2. Hydrogen Bonds and Crystal Packing of Polymorphs

The hydrogen bond motifs in the four ROY polymorphs are compared in Figure 3.

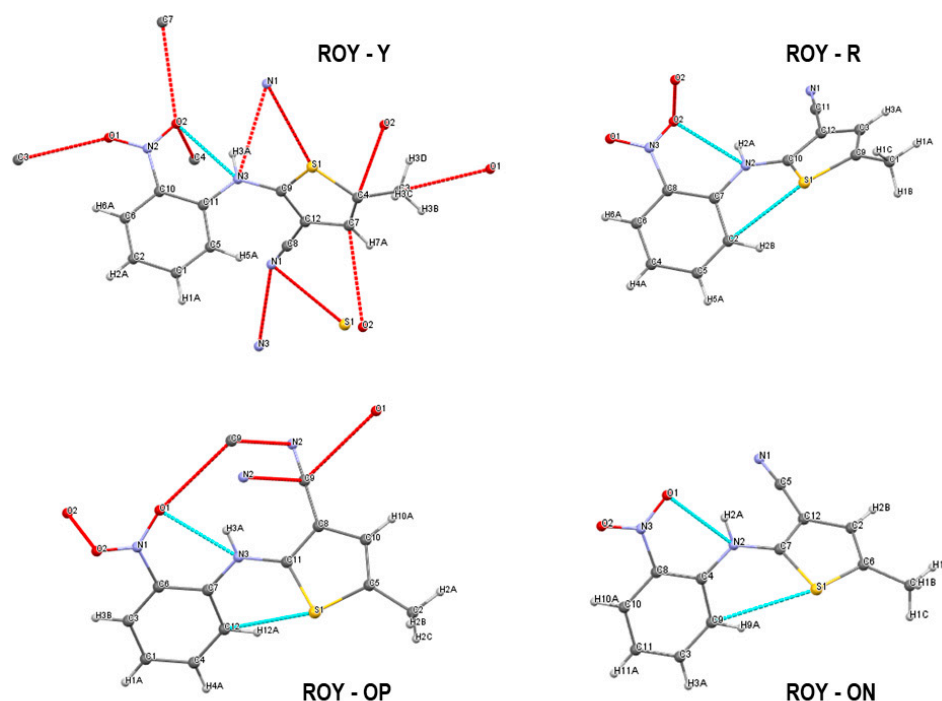


**Figure 3.** Hydrogen bonding motifs in different ROY polymorphs at 123 K. Polymorph Y has the largest number of intermolecular hydrogen bonds (red dotted lines), while polymorph ON has none. Intramolecular hydrogen bonds are shown as teal lines.

The thermal expansivity of the corresponding hydrogen bonds is tabulated in Table 2.

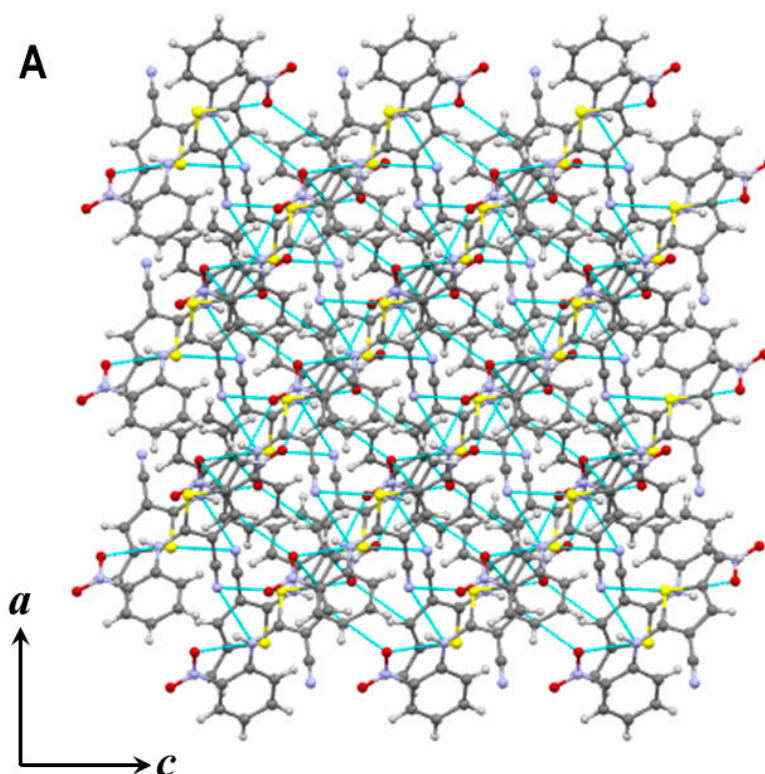


**Table 2.** Expansivity hierarchy of hydrogen bonds in ROY polymorphs at 123 K.

Polymorph	Hydrogen Bond	Bond Type	Bond Length (Å)	Bond Expansivity $\times 10^{-6} \text{ (K}^{-1})^*$
Y	N <sub>2</sub> ⋯ H–N <sub>1</sub>	Intermolecular	3.067	88.03
	S <sub>1</sub> ⋯ H–N <sub>2</sub>	Intermolecular	3.304	96.85
	O <sub>2</sub> ⋯ H–C <sub>9</sub>	Intermolecular	3.184	75.37
	O <sub>2</sub> ⋯ H–N <sub>1</sub>	Intramolecular	2.620	7.63
R	O <sub>2</sub> ⋯ H–O <sub>2</sub>	Intermolecular	2.936	66.07
	O <sub>2</sub> ⋯ H–N <sub>1</sub>	Intramolecular	2.634	−6.07
	S <sub>1</sub> ⋯ H–C <sub>2</sub>	Intramolecular	3.145	39.43
OP	O <sub>1</sub> ⋯ H–O <sub>1</sub>	Intermolecular	2.943	102.62
	O <sub>2</sub> ⋯ H–N <sub>1</sub>	Intramolecular	2.654	−18.84
	S <sub>1</sub> ⋯ H–C <sub>2</sub>	Intramolecular	3.239	30.26
ON	O <sub>2</sub> ⋯ H–N <sub>1</sub>	Intramolecular	2.616	−3.27
	S <sub>1</sub> ⋯ H–C <sub>2</sub>	Intramolecular	3.356	−59.59

\* Bond expansivity =  $\frac{(\delta x/\delta T)_p}{x}$  where  $x$  = bond length

In **polymorph Y**, several intermolecular hydrogen bond interactions with N–H and C–H as hydrogen bond donors are observed (Figure 3 and Table 2). These interactions are relatively weak (hydrogen bond with lengths  $>3 \text{ \AA}$ ) [33,34] and the bond length increases significantly with increasing temperature (Table 2). However, when these interactions work together while constructing the molecular packing in the Y polymorph, they create and fortify a dense hydrogen-bonded network along the  $a$  and  $c$  axes of polymorph Y (Figure 4A). Packing is visibly much less dense along axis  $b$ , where molecules are arranged in alternating dimers with no intermolecular hydrogen bond interactions running along direction  $b$  (Figure 4B). Interestingly, the maximum axial expansivity occurs along axis  $b$  in polymorph Y (Table 1), corresponding to the direction of less dense packing of molecules.

**Figure 4.** Cont.

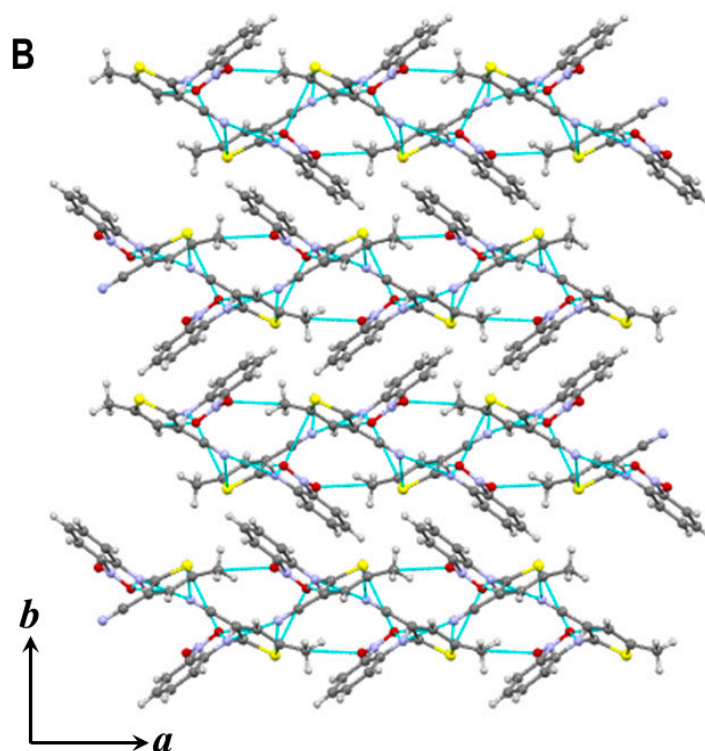


**Figure 4.** Crystal packing in polymorph Y showing (A) very dense hydrogen-bonded network along axes *a* and *c*, and (B) molecules arranged in alternating dimers with less dense packing along axis *b*. Weak hydrogen bonds are shown as teal lines.

In **polymorph OP**, there is a single moderately strong intermolecular O $\cdots$ H–O interaction (bond length  $\sim 2.9\text{\AA}$  at 123 K). In addition, there are a couple of intramolecular hydrogen bonds. The intramolecular hydrogen bonds in all four polymorphs show small expansivity. These interactions are not expected to majorly influence the overall volume expansivity of the unit cells. In this polymorph, molecules pack in flat hydrogen-bonded layers along the *bc* plane (Figure 5). The maximum expansivity is observed in the direction along the *a* axis (Table 1).

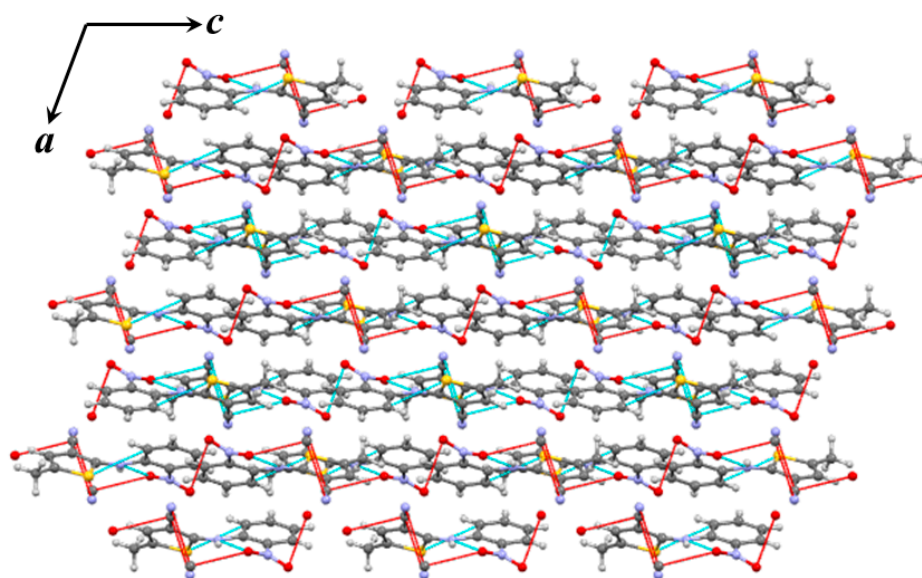


**Figure 5.** Crystal packing in polymorph OP showing hydrogen-bonded layers. Intermolecular (red lines) and intramolecular hydrogen bonds (teal lines) are shown.

In **polymorph ON**, the polymorph that displays the maximum volume expansivity, only intramolecular and no intermolecular hydrogen bonds could be identified (Figure 3). Molecules in this polymorph are packed into layers parallel to the  $bc$  plane perpendicular to axis  $a$  (Figure 6), which exhibits maximum expansivity (Table 1).

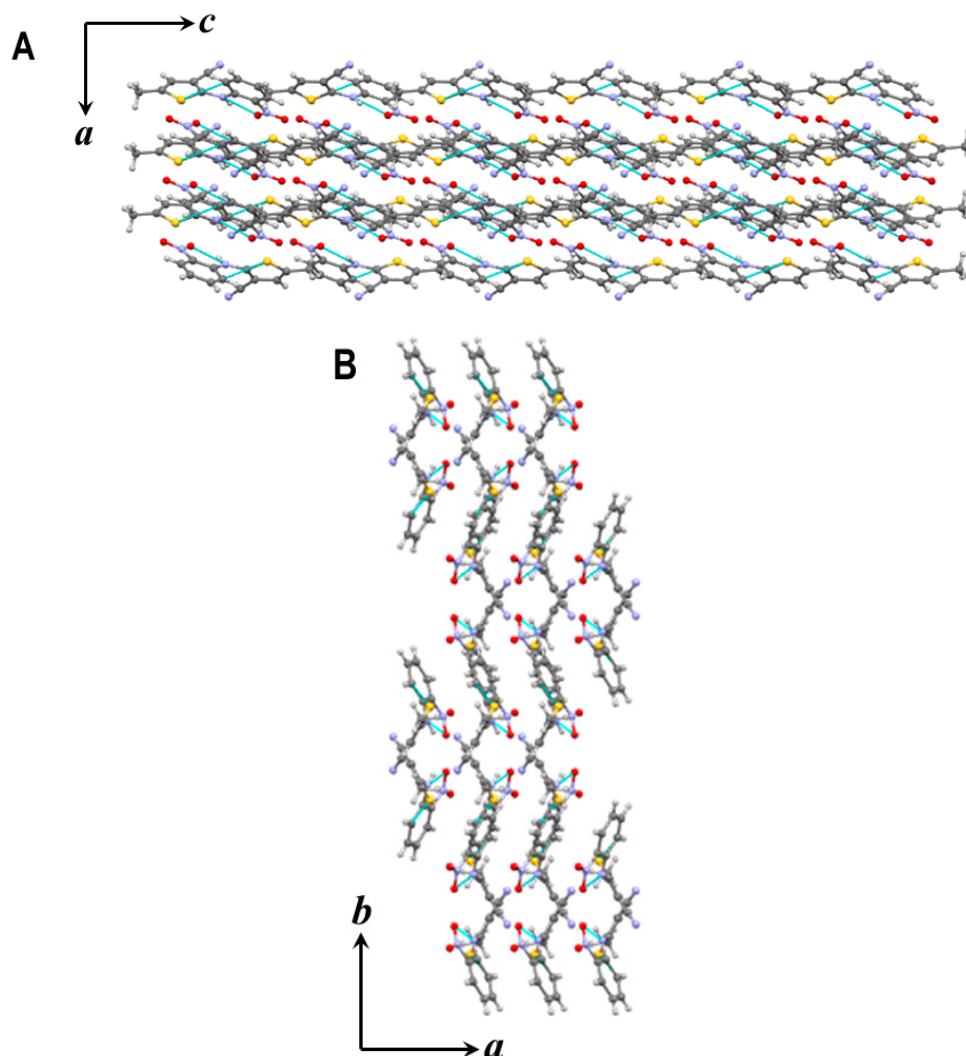


**Figure 6.** (A) Crystal packing in polymorph ON shows a layered structure along axes  $b$  and  $c$ . (B) The maximum expansion occurs in directions perpendicular to these layers (i.e., along axis  $a$ ), while the directions along the layers show much smaller expansivities.

In **polymorph R**, only one type of intermolecular hydrogen bond ( $O \cdots H-O$ ) is formed along with two intramolecular hydrogen bond interactions. Molecules are packed to form flat (100) layers in this crystal (Figure 7A). The direction of maximum axial expansivity is  $a$  (Table 1). Adjacent (100) layers are connected by the intermolecular  $O \cdots H-O$  hydrogen bond interactions (Figure 7B).

### 3.3. Crossover of Thermal Density Lines

Corresponding to linear volume expansion, the densities for the four ROY polymorphs decrease linearly with increasing temperature but with different slopes, i.e., different thermal density gradients (Figure 8). The rank order of the thermal density gradients (unit of  $\times 10^{-4} \text{ g mL}^{-1} \text{ K}^{-1}$ ) is 3.05 (ON) > 2.88 (OP) > 2.84 (R) > 2.34 (Y). A linear regression model best describes the relationship between crystal density and temperature, with a high R-square value of > 0.99 indicating an excellent fit for all four polymorphs. The thermal



density lines are projected to cross at  $\sim 83$  K for polymorph pair Y–R (monotropic pair), and  $\sim 17$  K for polymorph pair Y–OP (enantiotropic pair,  $T_t \sim 346$  K). No density crossover is expected between the polymorph ON, which consistently shows the lowest density over the entire temperature range of 0–300 K, and any of the other three polymorphs. The projected rank order for crystal densities at absolute zero is  $R (1.5247 \pm 0.0029 \text{ g/mL}) > OP (1.5215 \pm 0.0029 \text{ g/mL}) > Y (1.5206 \pm 0.0007 \text{ g/mL}) > ON (1.5189 \pm 0.0016 \text{ g/mL})$ , which is different from the density rank order at the room temperature  $Y (1.447 \text{ g/mL}) > R (1.438 \text{ g/mL}) > OP (1.435 \text{ g/mL}) > ON (1.428 \text{ g/mL})$ .

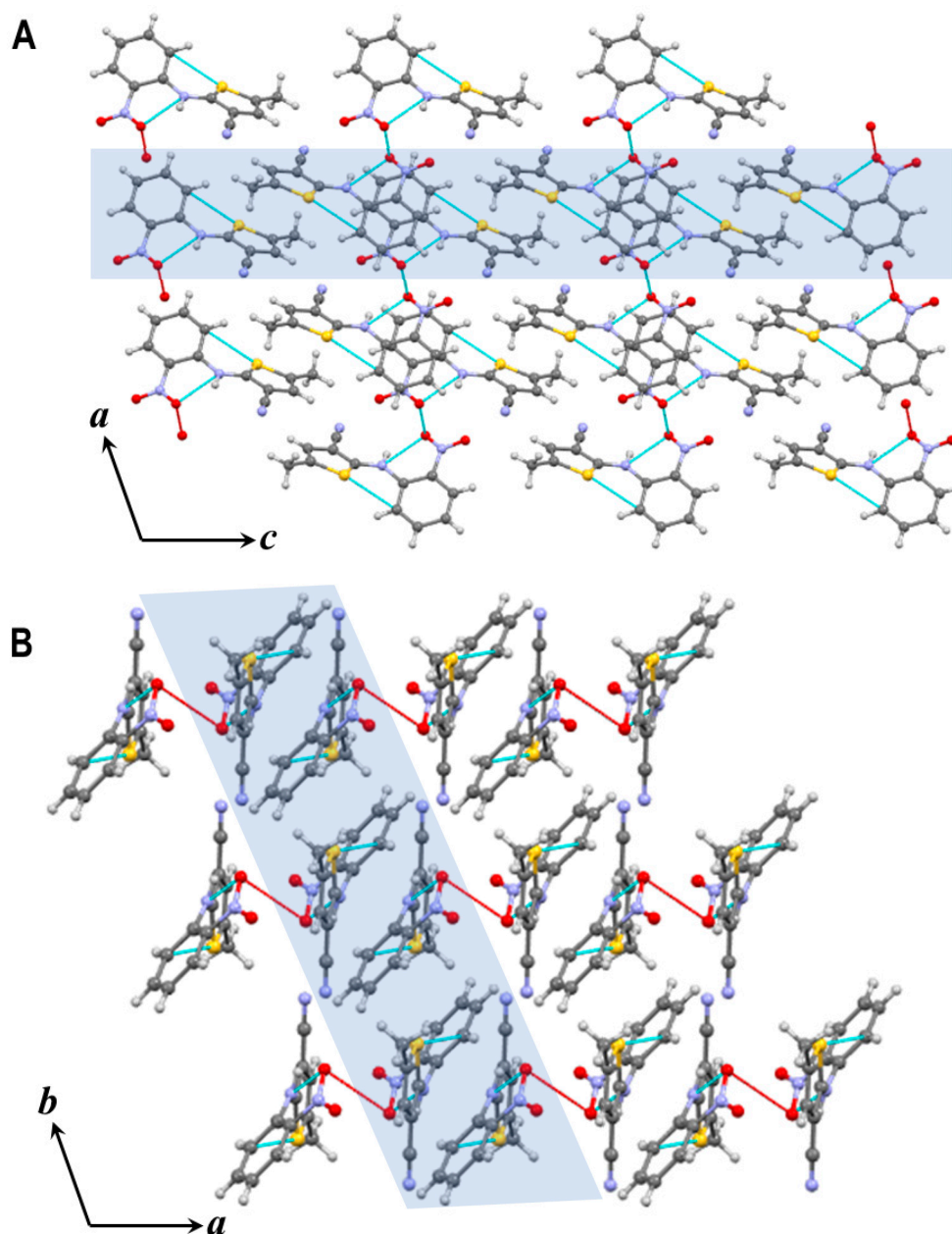


**Figure 7.** Crystal packing in polymorph R. (A) Viewed from the *b* axis; (B) viewed from the *c* axis. The shaded layer is (100).

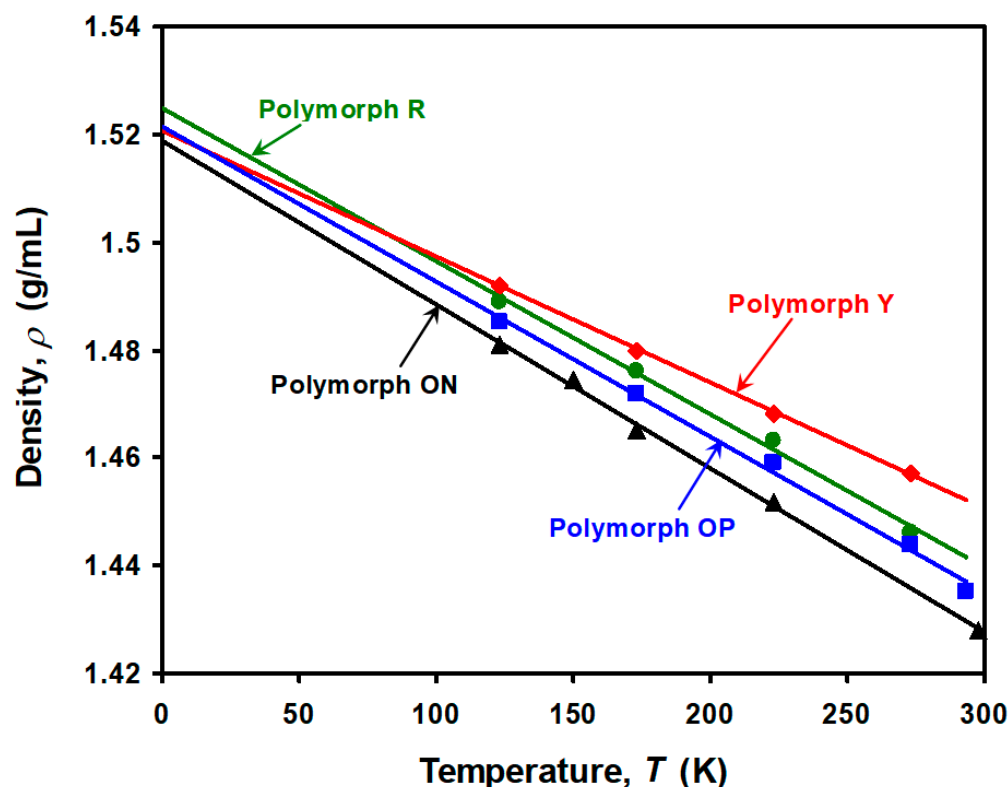


Figure 8. Thermal density profiles ( $\rho$ - $T$ ) of polymorphs Y, R, OP, and ON.

#### 4. Discussion

##### 4.1. Structure–Expansivity Correlations

The materials science tetrahedron (MST) entails that properties of a material are determined by its structure, which can be engineered to attain desired properties [35]. Strong correlations between the crystal structure and several properties, such as solubility [20,23], physicochemical stability [20,36], and mechanical performance [8,37–40], have been demonstrated. Even though the phenomenon of thermal expansion has been well-studied for a wide range of materials [9,17,18,41–43], its relationship with structures of molecular crystals has been relatively less explored [11,16,44,45]. This work has yielded new insights into the relationship between crystal structure and thermal expansion of molecular crystals.

The thermal expansivity of the four polymorphs of ROY studied in this work can be explained based on their crystal packing differences. Expansion is anisotropic in all cases, which corresponds to anisotropic molecular packing in these crystals. Volume expansivity ( $Y < OP \approx R < ON$ , Figure 2) shows an inverse dependence on the number of intermolecular hydrogen bonds:  $Y (3) > OP (1) = R (1) > ON (0)$ . Among the four polymorphs investigated, polymorph Y shows the lowest volume expansivity (Table 1), the smallest thermal density gradient ( $\delta\rho/\delta T$ ), and the densest network of intermolecular hydrogen bonds.

For the layered polymorphs (e.g., polymorph ON), the expansivity is the largest along the directions perpendicular to the layers. Similar observations were made in  $\beta$ -succinic acid, oxalic acid, and  $\alpha$ -adipic acid crystals [44,46], where the expansivity is the largest along the direction perpendicular to the layers and the smallest in the plane of the layers. Indeed, the largest overall volume expansion among the four polymorphs; hence, the absolute value of density change, is observed for polymorph ON, which has a flat, layered structure but without intermolecular hydrogen bonds. It should be noted that the absence of intermolecular hydrogen bonds in ON leads to a more energetically isotropic structure than the other three polymorphs, which is reflected by the relatively more uniform lattice expansion (Table 1).

In comparison to polymorph ON, the experimental volume expansivity of polymorph R is higher despite its similar layered structure. This is attributed to the presence of  $O \cdots H-O$  interactions between adjacent (100) layers, which leads to more resistance to expansion in the direction perpendicular to the layers. The contraction of the  $\alpha$  and  $\gamma$  unit cell angles in R is a consequence of the new force equilibrium among atoms to accommodate the large increase along the  $a$  axis to achieve overall positive thermal expansion. The contraction of a unit cell component on heating, though not as common as expansion, has been observed in structures involving metallophilic interactions [47], as well as organic molecular crystals [13,43].

#### 4.2. Density Crossover among Polymorphs

An important consequence of the different thermal expansivity of polymorphs is the possible violation of the density rule. Polymorph Y has the lowest free energy among the four ROY polymorphs below  $\sim 70$  °C [26,28]. At room temperature, polymorph Y has the highest density, and hence the closest packing, which is consistent with its thermodynamic stability. Thus, density is a good predictor of stability of Y with respect to other polymorphs at room temperature. However, the significant differences in the volume expansivities of the four polymorphs suggests the possibility of crossover of their thermal density lines (Figure 8). When density lines cross, the density rule is necessarily violated at a temperature either below or above the density crossover temperatures ( $T_d$ ), since the density order of polymorphs switches when temperature passes  $T_d$ . In fact, despite being the most thermodynamically stable, polymorph Y does not have the highest density at absolute zero, owing to the density crossover phenomenon (Figure 8).

Polymorph R is predicted to have the highest density at absolute zero when applying linear regression analysis to thermal density data. However, it has been shown that the relationship between  $V$  and  $T$  sometimes may deviate from linearity for inorganic atomic crystals at very low temperatures (typically  $<30$  K) because individual atomic vibrations assume a cubic temperature variation as temperature approaches absolute zero [9]. A linear extrapolation of the density gradient is used here as most molecular organic crystals show linear density gradients up to temperatures very close to 0 K based on an analysis of crystal structures in the Cambridge Structure Database (CSD) [16]. Although deviations of the thermal density lines from linearity affect  $T_d$ , violation of the density rule is inevitable as long as the thermal density lines cross.

This density crossover phenomenon is independent of thermodynamic stability relationships (i.e., enantiotropic or monotropic) between two polymorphs. For example, the density lines cross for both the monotropic Y–R pair at  $\sim 83$  K and the enantiotropic Y–OP pair at  $\sim 17$  K. Therefore, for the enantiotropic Y–OP pair, the density rule is valid only within the temperature range bracketed by the temperatures of density crossover ( $T_d = \sim 17$  K) and thermodynamic transition ( $T_t = 346$  K). For the monotropic Y–R pair, the density rule is valid above the density crossover temperature of  $\sim 83$  K.

Thus, the use of density rule for predicting the thermodynamic stability of polymorphs requires the consideration of thermal density functions of the polymorphs. The use of only density values of polymorphs at a single temperature is less reliable than the use of thermal density functions. At a minimum, when applying the density rule, crystal packing features should be considered where structures containing a denser hydrogen bond network tend to be more resistant to thermal expansion. Thus, a polymorph with a lower density at a given temperature and exhibiting a stronger lattice, e.g., presence of a denser hydrogen bond network, likely retains its lower density at absolute zero because of its slower rise in density with decreasing temperature. Therefore, the density rule should be applied with greater caution, since failed cases are many, especially when the crystal packing is dominated by hydrogen bonding [20,21,48]. As shown by polymorph R, a polymorph with a higher density at absolute zero may not necessarily be the most thermodynamically stable form [16]. It should also be mentioned that the density rule may fail even in the absence of the thermal density gradient crossover phenomenon. An example of such

violation is the case of acetaminophen polymorphs I and II. The thermodynamically stable acetaminophen polymorph I is consistently less dense at all temperatures up to 0 K, which is again attributed to the differences in the strengths of hydrogen bond interactions in the two polymorphs [48].

Mechanistically, the impact of crystal density (or volume) on polymorph stability is linked to its effect on the rank order of free energy ( $\Delta G$ ) of polymorphs. Under constant pressure ( $P$ ) at 0 K,  $\Delta G$  is equivalent to the rank order of the crystal enthalpies ( $\Delta H$ ), which is dependent on the differences in both internal energies of polymorphs ( $\Delta U$ ) and the cell volumes ( $\Delta V$ ) or densities, since  $\Delta H = \Delta U + P\Delta V$  [49]. Thus, both internal energy and density differences among polymorphs contribute to their different thermodynamic stabilities. The difference in crystal packing, in particular the number and type of hydrogen bonds among polymorphs, contribute to differences in both density and  $\Delta U$ .

## 5. Conclusions

Thermal expansion, a fundamental physical property of materials, has received limited exploration for polymorphs of molecular crystals. In this study, we established the qualitative relationships between the thermal expansivity of four ROY polymorphs and their crystal-packing patterns. Thermal expansivity is highly anisotropic in all four ROY polymorphs, which is consistent with their structural anisotropy. A layered molecular packing pattern seems to favor overall volume expansion of the lattice, while the presence of a dense hydrogen-bonded molecular network hinders it. These observations suggest that directional hydrogen-bonding interactions are more resistant to thermal expansion than nondirectional *van der Waals'* interactions. The phenomenon of thermal expansion complicates the application of the density rule in predicting stability relationships among polymorphs. Thermal density functions of different polymorphs can cross, leading to the temperature dependence of the rank order of their density. As such, it is risky to determine stability relationships of polymorphs based on density values determined at a single temperature, especially if it is far away from the temperature of interest. Despite being the most stable polymorph at absolute zero, polymorph Y does not have the highest density, owing to the density crossover phenomenon resulting from the different thermal expansivities of ROY polymorphs.

**Supplementary Materials:** Summary of crystal structure solution parameters at different temperatures for the polymorphs are provided in the supporting information. The following supporting information can be downloaded at: <https://www.mdpi.com/article/10.3390/cryst13020270/s1>.

**CCDC Reference Numbers:** 2232906 (OP—123K); 2232907 (OP—173K); 2232908 (OP—223K); 2232909 (OP—273K); 2232910 (R—173K); 2232911 (R—173K); 2232912 (R—223K); 2232913 (R—273K); 2232937 (Y—123K); 2232938 (Y—173K); 2232936 (Y—223K); 2232939 (Y—273K); 2232903 (ON—123K).

**Author Contributions:** Conceptualization, C.C.S.; Methodology, C.C.S.; Formal analysis, S.C.; Investigation, S.C.; Resources, C.C.S.; Data curation, S.C.; Writing—original draft, S.C.; Writing—review & editing, C.C.S.; Supervision, C.C.S.; Funding acquisition, C.C.S. All authors have read and agreed to the published version of the manuscript.

**Funding:** S.C. is grateful for a David and Marilyn Grant Fellowship in Physical Pharmacy (2010–2011) and a University of Minnesota Graduate School Doctoral Dissertation Fellowship (2011–2012).

**Acknowledgments:** Crystal structure data were collected at the X-ray Crystallography Laboratory, S146 Kolthoff Hall, Department of Chemistry, University of Minnesota. We thank Byoung Hwa Son for growing the single crystals of the ROY polymorphs.

**Conflicts of Interest:** The authors declare no conflict of interest.

## References

1. Verma, A.R.; Krishna, P. *Polymorphism and Polytypism in Crystals*; John Wiley & Sons: New York, NY, USA, 1966.
2. Bernstein, J. *Polymorphism in Molecular Crystals*; Oxford University Press: New York, NY, USA, 2002.
3. Byrn, S.R. *Solid State Chemistry of Drugs*; Academic Press: New York, NY, USA, 1982.

4. Brittain, H.G. (Ed.) *Polymorphism in Pharmaceutical Solids*; Marcel Dekker: New York, NY, USA, 1999.
5. Borka, L.; Haleblan, J.K. Crystal polymorphism of pharmaceuticals. *Acta Pharm. Jugosl.* **1990**, *40*, 71–94.
6. Haleblan, J.K. Characterization of habits and crystalline modification of solids and their pharmaceutical applications. *J. Pharm. Sci.* **1975**, *64*, 1269–1288. [[CrossRef](#)] [[PubMed](#)]
7. Datta, S.; Grant, D.J.W. Crystal structures of drugs: Advances in determination, prediction and engineering. *Nat. Rev.* **2004**, *3*, 42–57. [[CrossRef](#)] [[PubMed](#)]
8. Sun, C.C.; Grant, D.J.W. Influence of Crystal Structure on the Tableting Properties of Sulfamerazine Polymorphs. *Pharm. Res.* **2001**, *18*, 274–280. [[CrossRef](#)]
9. Taylor, R.E. *Thermal Expansion of Solids*; Ho, C.Y., Ed.; ASM International: Materials Park, OH, USA, 1998; Volume I-4.
10. Taylor, R.E.; Denman, G.L. (Eds.) *Thermal Expansion*; American Institute of Physics: New York, NY, USA, 1974.
11. Das, D.; Jacobs, T.; Pietraszko, A.; Barbour, L.J. Anomalous thermal expansion of an organic crystal—Implications for elucidating the mechanism of an enantiotropic phase transformation. *Chem. Commun.* **2011**, *47*, 6009–6011. [[CrossRef](#)]
12. Liang, E.; Sun, Q.; Yuan, H.; Wang, J.; Zeng, G.; Gao, Q. Negative thermal expansion: Mechanisms and materials. *Front. Phys.* **2021**, *16*, 53302. [[CrossRef](#)]
13. Lee, A.v.d.; Dumitrescu, D.G. Thermal expansion properties of organic crystals: A CSD study. *Chem. Sci.* **2021**, *12*, 8537–8547.
14. Salvador, J.R.; Guo, F.; Hogan, T.; Kanatzidis, M.G. Zero thermal expansion in YbGaGe due to an electronic valence transition. *Nature* **2003**, *425*, 702–705. [[CrossRef](#)]
15. Margadonna, S.; Prassides, K.; Fitch, A.N. Zero Thermal Expansion in a Prussian Blue Analogue. *J. Am. Chem. Soc.* **2004**, *126*, 15390–15391. [[CrossRef](#)]
16. Sun, C.C. Thermal Expansion of Organic Crystals and Precision of Calculated Crystal Density: A Survey of Cambridge Crystal Database. *J. Pharm. Sci.* **2007**, *96*, 1043–1052. [[CrossRef](#)]
17. Fortes, A.D.; Suard, E.; Knight, K.S. Negative Linear Compressibility and Massive Anisotropic Thermal Expansion in Methanol Monohydrate. *Science* **2011**, *331*, 742–745. [[CrossRef](#)] [[PubMed](#)]
18. Grima, J.N.; Attard, D.; Gatt, R. Unusual Thermoelastic Properties of Methanol Monohydrate. *Science* **2011**, *331*, 687–688. [[CrossRef](#)]
19. White, G.K.; Choy, C.L. Thermal expansion and Grüneisen parameters of isotropic and oriented polyethylene. *J. Polym. Sci. Polym. Phys. Ed.* **1984**, *22*, 835–846. [[CrossRef](#)]
20. Burger, A.; Ramberger, R. On the Polymorphism of Pharmaceuticals and Other Molecular Crystals. I Theory of Thermodynamic Rules. *Mikrochim. Acta* **1979**, *72*, 259–271. [[CrossRef](#)]
21. Burger, A.; Ramberger, R. On the Polymorphism of Pharmaceuticals and Other Molecular Crystals. II Applicability of Thermodynamic Rules. *Mikrochim. Acta* **1979**, *72*, 273–316. [[CrossRef](#)]
22. Westrum, E.F.; McCullough, J.P. *Thermodynamics of Crystals*; Interscience Publishers: New York, NY, USA, 1963.
23. Grant, D.J.W.; Higuchi, T. *Solubility Behavior of Organic Compounds*; John Wiley & Sons: New York, NY, USA, 1990.
24. Perumalla, S.R.; Wang, C.; Guo, Y.; Shi, L.; Sun, C.C. Robust bulk preparation and characterization of sulfamethazine and saccharine salt and cocrystal polymorphs. *Cryst. Eng. Commun.* **2019**, *21*, 2089–2096. [[CrossRef](#)]
25. Yu, L. Inferring Thermodynamic Stability Relationship of Polymorphs from Melting Data. *J. Pharm. Sci.* **1995**, *94*, 966–974. [[CrossRef](#)] [[PubMed](#)]
26. Yu, L.; Stephenson, G.A.; Mitchell, C.A.; Bunnell, C.A.; Snorek, S.V.; Bowyer, J.B.; Borchardt, T.B.; Stowell, J.G.; Byrn, S.R. Thermochemistry and Conformational Polymorphism of a Hexamorphic Crystal System. *J. Am. Chem. Soc.* **2000**, *122*, 585–591. [[CrossRef](#)]
27. Yu, L.; Huang, J.; Jones, K.J. Measuring Free-Energy Difference between Crystal Polymorphs through Eutectic Melting. *J. Phys. Chem. B* **2005**, *109*, 19915–19922. [[CrossRef](#)]
28. Chen, S.; Guzei, I.A.; Yu, L. New polymorphs of ROY and new record for coexisting polymorphs of solved structures. *J. Am. Chem. Soc.* **2005**, *127*, 9881–9885. [[CrossRef](#)]
29. Yao, Z.S.; Guan, H.; Shiota, Y.; He, C.T.; Wang, X.L.; Wu, S.Q.; Zheng, X.; Su, S.Q.; Yoshizawa, K.; Kong, X.; et al. Giant anisotropic thermal expansion actuated by thermodynamically assisted reorientation of imidazoliums in a single crystal. *Nat. Commun.* **2019**, *10*, 4805. [[CrossRef](#)] [[PubMed](#)]
30. Janiak, A.; Esterhuysen, C.; Barbour, L.J. A thermo-responsive structural switch and colossal anisotropic thermal expansion in a chiral organic solid. *Chem. Commun.* **2018**, *54*, 3727–3730. [[CrossRef](#)] [[PubMed](#)]
31. Bhattacharya, S.; Saha, B.K. Steric guided anomalous thermal expansion in a dimorphic organic system. *CrystEngComm* **2014**, *16*, 2340–2343. [[CrossRef](#)]
32. Ding, X.; Crawford, A.W.; Derrick, W.P.; Unruh, D.K.; Groeneman, R.H.; Hutchins, K.M. Thermal Expansion Properties and Mechanochemical Synthesis of Stoichiometric Cocrystals Containing Tetrabromobenzene as a Hydrogen- and Halogen-Bond Donor. *Chem. Eur. J.* **2021**, *27*, 16329–16333. [[CrossRef](#)]
33. Desiraju, G.R. The C-H ··· O Hydrogen Bond: Structural Implications and Supramolecular Design. *Acc. Chem. Res.* **1996**, *29*, 441–449. [[CrossRef](#)]
34. Desiraju, G.R. Hydrogen Bridges in Crystal Engineering: Interactions without Borders. *Acc. Chem. Res.* **2002**, *35*, 565–573. [[CrossRef](#)] [[PubMed](#)]



35. Sun, C.C. Materials science tetrahedron—a useful tool for pharmaceutical research and development. *J. Pharm. Sci.* **2009**, *98*, 1671–1687. [[CrossRef](#)]
36. Chen, X.; Stowell, J.G.; Morris, K.R.; Byrn, S.R. Quantitative study of solid-state acid–base reactions between polymorphs of flufenamic acid and magnesium oxide using X-ray powder diffraction. *J. Pharm. Biomed. Anal.* **2010**, *51*, 866–874. [[CrossRef](#)]
37. Chatteraj, S.; Shi, L.; Sun, C.C. Understanding the relationship between crystal structure, plasticity and compaction behaviour of theophylline, methyl gallate, and their 1:1 co-crystal. *Cryst. Eng. Comm.* **2010**, *12*, 2466–2472. [[CrossRef](#)]
38. Wang, K.; Mishra, M.K.; Sun, C.C. Exceptionally Elastic Single-Component Pharmaceutical Crystals. *Chem. Mater.* **2019**, *31*, 1794–1799. [[CrossRef](#)]
39. Hu, S.; Mishra, M.K.; Sun, C.C. Twistable Pharmaceutical Crystal Exhibiting Exceptional Plasticity and Tabletability. *Chem. Mater.* **2019**, *31*, 3818–3822. [[CrossRef](#)]
40. Zhang, K.; Sun, C.C.; Liu, L.; Wang, C.; Shi, P.; Xu, J.; Wu, S.; Gong, J. Structural Origins of Elastic and 2D Plastic Flexibility of Molecular Crystals Investigated with Two Polymorphs of Conformationally Rigid Coumarin. *Chem. Mater.* **2021**, *33*, 1053–1060. [[CrossRef](#)]
41. Brand, H.E.A.; Fortes, A.D.; Wood, I.G.; Knight, K.S.; Vocadlo, L. The thermal expansion and crystal structure of mirabilite ( $\text{Na}_2\text{SO}_4 \cdot 10\text{D}_2\text{O}$ ) from 4.2 to 300 K, determined by time-of-flight neutron powder diffraction. *Phys. Chem. Miner.* **2009**, *36*, 29–46. [[CrossRef](#)]
42. Fortes, A.D.; Wood, I.G.; Knight, K.S. The crystal structure and thermal expansion tensor of  $\text{MgSO}_4 \cdot 11\text{D}_2\text{O}$  (meridianiite) determined by neutron powder diffraction. *Phys. Chem. Miner.* **2008**, *35*, 207–221. [[CrossRef](#)]
43. Das, D.; Jacobs, T.; Barbour, L.J. Exceptionally large positive and negative anisotropic thermal expansion of an organic crystalline material. *Nat. Mater.* **2010**, *9*, 36–39. [[CrossRef](#)]
44. Amoros, J.L.; Canut, M.L.; Neira, E. Thermal Expansion of  $\beta$ -Succinic Acid and  $\alpha$ -Adipic Acid in Relation to Their Crystal Structures. *Proc. Royal Soc. Lond. Ser. A* **1965**, *285*, 370–381.
45. Stephenson, G.A. Anisotropic lattice contraction in pharmaceuticals: The influence of cryo-crystallography on calculated powder diffraction patterns. *J. Pharm. Sci.* **2006**, *95*, 821–827. [[CrossRef](#)] [[PubMed](#)]
46. Wang, C.; Sun, C.C. Computational Techniques for Predicting Mechanical Properties of Organic Crystals: A Systematic Evaluation. *Mol. Pharm.* **2019**, *16*, 1732–1741. [[CrossRef](#)] [[PubMed](#)]
47. Korcok, J.L.; Katz, M.J.; Leznoff, D.B. Impact of Metallophilicity on “Colossal” Positive and Negative Thermal Expansion in a Series of Isostructural Dicyanometallate Coordination Polymers. *J. Am. Chem. Soc.* **2009**, *131*, 4866–4871. [[CrossRef](#)]
48. Nelyubina, Y.V.; Glukhov, I.V.; Antipin, M.Y.; Lyssenko, K.A. “Higher density does not mean higher stability” mystery of paracetamol finally unraveled. *Chem. Commun.* **2010**, *46*, 3469–3471. [[CrossRef](#)]
49. Van Wylen, G.J.; Sonntag, R.E. *Fundamentals of Classical Thermodynamics*, 3rd ed.; John Wiley & Sons: New York, NY, USA, 1985.

**Disclaimer/Publisher’s Note:** The statements, opinions and data contained in all publications are solely those of the individual author(s) and contributor(s) and not of MDPI and/or the editor(s). MDPI and/or the editor(s) disclaim responsibility for any injury to people or property resulting from any ideas, methods, instructions or products referred to in the content.